ISSN 1068-3755, Surface Engineering and Applied Electrochemistry, 2020, Vol. 56, No. 1, pp. 112–125. © Allerton Press, Inc., 2020.

Corrosion Resistance and Cathodic Disbondment of Epoxy Coating Applied on Zinc Phosphate Conversion Coating Containing Different Amounts of Cobalt Ions

R. Hosseinirad[a], *, M. Toorani[a], and A. Sabour Rouhaghdam[a]

[a] *Department of Materials Engineering, Tarbiat Modares University, Tehran, Iran*

**e-mail: rad.reza1371@rocketmail.com*

Received May 2, 2019; revised July 17, 2019; accepted July 17, 2019

Abstract—In this study, the influence of phosphate surface pretreatment containing a cobalt ion additive on the anti-corrosion features of epoxy coating was investigated. Phosphate conversion coating (PCC) specimens were prepared. Then the epoxy coating was electrostatically sprayed on the phosphated substrate. The surface morphology and the composition of a zinc phosphate conversion coating with a cobalt ion additive were studied by scanning electron microscopy and X-ray diffraction, respectively. Also, the corrosion protection properties of specimens were studied by the polarization potentiodynamic test in 3.5% NaCl solution. Protective performance of double-layer coatings was studied using electrochemical impedance spectroscopy during 30 days in the mentioned solution. In addition, the impact of phosphate chemical treatment on increasing the adhesion strength of the powder coating was studied using the pull-off adhesion test and cathodic disbodnment test in the same solution. As a result, it was found that the corrosion resistance of PCC containing a cobalt additive enhanced significantly and that the PCC containing 3 g/L Co is less porous than other coatings. Also, the protection properties, adhesion strength, and cathodic disbondment resistance of the double-layer coatings with phosphate pretreatment containing 3 g/L Co increased significantly.

Keywords: phosphate conversion coating, cathodic disbondment, double-layer coating, electrochemical impedance spectroscopy, pretreatment

DOI: 10.3103/S1068375520010081

INTRODUCTION

Epoxy coatings due to excellent corrosion resistance, high chemical stability, and good adhesion strength are applied on the surface of steel to protect it in corrosive environments. Electrostatic powder coatings are environmentally friendly, economical, and have excellent coating properties [1, 2]. One of the disadvantages of epoxy coatings is their permeability when exposed to corrosive solutions [3–10]. Water molecules penetrating into the coating and reaching the coating/substrate interface lead to a decrease in adhesion of organic coatings [4–6, 8]. Coating adhesion strength can be improved due to mechanical interlocking and chemical bonding between the film and the bare metal. In order to achieve better surface to increase its adhesion strength, all pollutants such as corrosion products and metal oxides should be removed from the surface. Based on the pores shape, the roughness, and contact angle of the wetting of the metal substrate will be affected. One of the strategies to increase the bond strength of organic coatings and improve the protection properties is the use of conversion coatings as surface pre-treatment. Generally, when using these coatings, both physical and mechanical bondings will increase on the surface, which will improve adhesion strength. In addition, changing the amount of the free surface energy and of roughness has a significant impact on the adhesion bonds in the coating/substrate interface [4, 5].

Phosphate conversion coating (PCC) is used because of economical reasons: it is easy to apply, it has good corrosion resistance, high adhesion strength, and high lubricity rate [11]. In recent studies, low immersion temperature and time have been considered for the process to be cost-effective. Also, with the preservation of the above mentioned conditions, PCC should have good anti-corrosion properties [12–14]. Accelerator additives are a solution for modifying PCC properties at low temperatures, so that corrosion resistance is also provided. It has been reported that PCCs with a dense structure, fewer pores, and high corrosion resistance could be obtained by supplementing such additives as Ni^{2+}, Mn^{2+}, Ca^{2+}, etc. [15–18].

According to the research done elsewhere, anti-corrosion properties and morphology of coatings are affected by replenishing cation additives [19–21]. The impact of Mn^{2+} and Ni^{2+} ions on the phosphate deposited on Al 2024 alloy was studied in [13, 22]

Table 1. Composition of phosphate solution

	Samples name				
Composition	PZn	PZnCo	PZn_2Co	PZn_3Co	PZn_4Co
Phosphoric acid, mL/L	10	10	10	10	10
Nitric acid, mL/L	3	3	3	3	3
Zinc oxide, g/L	5.6	5.6	5.6	5.6	5.6
Sodium nitride, g/L	1.2	1.2	1.2	1.2	1.2
Sodium fluoride, g/L	0.3	0.3	0.3	0.3	0.3
Cobalt nitrate, g/L	–	1	2	3	4

whose authors found that additives decreased the phosphate crystals size, this phenomena being more common for Mn^{2+} additive. Also the coatings containing Mn additives are thicker, which leads to an increase in the coatings corrosion resistance. The corrosion resistance of PCCs containing nickel and niobium was studied in [23]. Regarding the mechanism of forming PCCs, a niobium additive has a greater impact on the protective performance. In general, additives can affect the grain size, thickness, and microstructure of conversion coatings. It was shown that adding cobalt ions to chromate conversion coatings leads to an improved corrosion resistance of zinc [24]. Hence, Co^{2+} can be a suitable option to improve the corrosion resistance of PCCs.

Another noticeable point is that conversion coatings can be utilized as surface pretreatment so as to improve adhesion strength and enhance the barrier properties of epoxy coatings [25]. As was reported elsewhere, PCC applied on the galvanized steel increased the adhesion strength of organic coatings [4, 5] as well as of a chromate conversion coating [8]. The influence of zirconium conversion coating as a pretreatment on the adhesion strength and the cathodic disbondment of an organic top layer was evaluated in [26] and it was shown that surface pretreatment improved the barrier properties, cathodic disbondment resistance, and adhesion strength of epoxy coatings. The synergetic effect of adding cobalt and nickel to PCCs on the adhesion strength and anti-corrosion properties of the top layer was studied in [1]. The results showed that PCC pretreatment containing a mixture of cobalt and nickel additives, through mechanical bonding with a limiting surface for performing cathodic reactions in the substrate/coating interface, led to an increase in adhesion strength and protective performance.

In this study, the influence of cobalt ion in PCC on the anti-corrosion properties of the top layer was investigated. Then the effect of this coating (PCC) as surface pretreatment on the corrosion resistance, cathodic disbondment, and adhesion strength of epoxy coatings deposited on steel was evaluated. The surface morphology and PCC composition were investigated by scanning electron microscopy (SEM) and x-ray diffraction (XRD), respectively. To analyze the corrosion performance of PCC, potentiodynamic polarization was used in 3.5% NaCl solution. To investigate the effect of phosphate surface pre-treatment and the effect of cobalt ions on the anti-corrosion properties of epoxy coating, an analysis of electrochemical impedance spectroscopy (EIS) at different times was carried out and cathodic disbondment and pull-off adhesion tests were used.

MATERIALS AND METHODS

Materials and Samples Preparation

Steel plates with dimensions of 7 × 10 × 0.5 cm as substrates were abraded by 800 sandpaper and then degreased for 10 minutes with ultrasonic in an acetone solution. After immersion of the samples in a solution of 5 vol % H_2SO_4, pickling happened. Then they were washed by deionized water and dried in air. Phosphoric acid, nitric acid, and sodium hydroxide (for pH adjustment) an ZnO, NaF, and $NaNO_2$ were used as purchased.

Preparation of PCC Solution

PCCs containing four different concentrations of cobalt ions (1, 2, 3, 4 g/L) and non-additive coating were prepared (see Table 1). By adjusting the pH at 2–2.5, surface treatment was performed. The deposition of a coating on samples was performed at 85 ± 5°C for 10 minutes. By adding cobalt, the pH was kept constant in the mentioned range and the samples were dried in air after surface treatment.

Surface Morphology and XRD Analysis

In order to evaluate the surface morphology of PCCs, SEM was used as well as XRD (for PCC composition) with the energy of 40 kV and a cobalt lamp with K_α radiation with the scanning speed 10 deg/min.

Electrostatic Spray of Coatings

After performing the surface pretreatment of PCC, for the deposition of an epoxy powder coating on a

steel substrate with and without PCC, the IRIS Electrostatic Dispenser equipped with a Corona model with a 100 kV DC source was used. Powder coatings were cured at 190°C for 15 min.

Anti-corrosion Performance Evaluation

Potentiodynamic polarization and EIS tests were performed on the PCC-treated steel samples and epoxy-coated steel specimens by a Potentiostat/Galvanostat (EG&G-A273) equipped with a frequency response analyzer.

A three-electrode corrosion system equipped with an auxiliary platinum electrode, a calomel saturation electrode as reference electrode, and coated samples as working electrode was used. 1 cm^2 of the coated samples was exposed to corrosive solution. The polarization test was done from −250 to 500 mV_{SCE} (Standard Calomel Electrode) at a scanning rate of 1 mV/s. Powersuite software was used to analyze the polarization test results. EIS test was performed for double-layer coatings in a frequency range of 65 kHz–0.01 Hz and a voltage range of ±10 mV AC. EIS test for double-layer coatings was performed in a 3.5% NaCl solution for 30 days in different immersion times. Finally, the Nyquist and Bod plots from the impedance data were analyzed by Zview2 software. The impedance test was repeated thrice for all samples.

Cathodic Disbondment Measurements

In order to study the cathodic disbondment, an artificial hole (diameter: 6 mm) was carefully created at the center of each coating specimen. The experiments were carried out at a cathodic potential of −1.6 V_{SCE} using Mg ingot as a sacrificial anode in a 3.5% NaCl solution. To prevent solvent penetration, the back and edges of the samples were insulated using beeswax and then the specimens were placed vertically inside the compartment. For all specimens, ten immersion times were repeated for up to 60 hours. To determine the disbonded area, the disbonded coating was removed with a sharp knife and then the radial cross-sections were considered from the center of the coating hole. This test was repeated thrice, for all coated specimens.

Pull-off Adhesion Test

Pull-off adhesion test was done on the coated specimens with and without PCC pretreatment both in a dry state and after 14 days of immersion in a 3.5% NaCl solution using Defelsko Positest according to ASTM-D4541. The diameter of the dolly used in this test was 20 mm; it was fixed on the surface of the coating using a cyanoacrylate glue. After baking glue, the strain was applied at a constant rate of 5 mm/min using the pull-off equipment till removing the epoxy coating from the substrate surface. As in other tests, this one was repeated thrice.

RESULTS AND DISCUSSION

Surface Characteristics and Phase Composition of PCCs

In order to investigate the effect of a cobalt ion additive on PCCs, the surface morphology of these coatings was evaluated. SEM images for the samples containing cobalt additive are shown in Fig. 1.

Figure 1a shows that a PCC without an additive has more cracks than other samples. When adding Co, the amount of cracks in the coating structure decreased, the lowest being observed for the sample containing 3 g/L ion cobalt (Fig. 1d). The structure of phosphate crystals based on the obtained results is mainly in the form of plate and mud. PCCs containing additives have a smoother texture than those without additives, so that the greatest plate-shaped structures were observed for the sample containing 3 g/L ions of Co. Therefore, changing the amount of plate-shaped structures, basing on the surface morphology, leads to an increase in the size of phosphate crystals for specimens containing cobalt [27]. When adding cobalt, the phosphate crystals formed on zinc become more uniform and less porous.

The densest coating of the PCC samples was obtained with 3 g/L ions of cobalt. However, the excessive addition of additive (4 g/L), due to the PCC formation mechanism (referred to in the following sections), created a heterogeneous and more porous layer. In a zinc phosphate bath, when the substrate is immersed in a phosphate solution, iron is dissolved in the micro-anode zone (formula (1)) and the hydrogen gas is released:

$$Fe + 2H^+ \rightarrow Fe^{2+} + H_2\uparrow . \quad (1)$$

The release of hydrogen occurs in the micro-cathode areas, which leads to an increase in the pH value in the metal/solution interface; this ends with a change in the solution charge balance, and consequently, the formation of PO_4^{3-}:

$$\begin{aligned} &H_3PO_4 \rightarrow H_2PO_4^- \\ &\rightarrow HPO_4^{2-} + 2H^+ \rightarrow PO_4^{3-} + 3H^+. \end{aligned} \quad (2)$$

The formed PO_4^{3-} reacted with dissolved iron ions, giving phosphophyllite according to the following formula:

$$\begin{aligned} &2PO_4^{3-} + Fe^{2+} + 2Zn^{2+} + 4H_2O \\ &\rightarrow Zn_2Fe(PO_4)_2 \cdot 4H_2O\downarrow . \end{aligned} \quad (3)$$

The $Zn_2Fe(PO_4)_2 \cdot 4H_2O$ phase is known to be a phosphophyllite phase that precipitates on the substrate surface. When the concentration of PO_4^{3-} ions in the bath reaches their saturation level, the formation of non-solvent metal phosphate begins in accordance

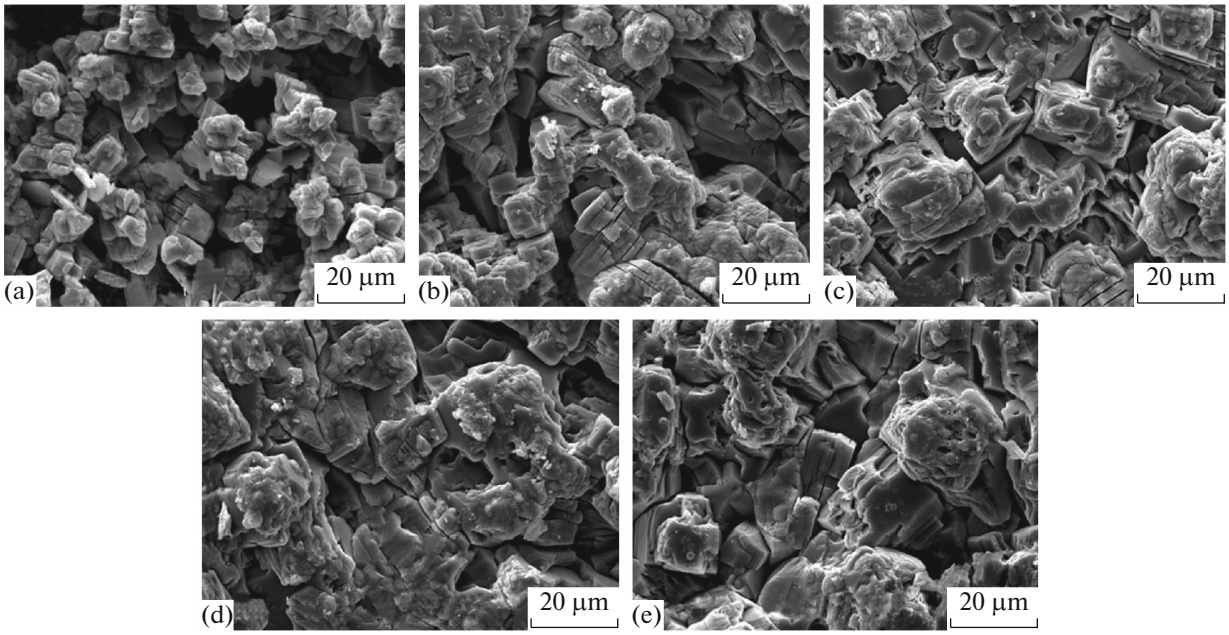

Fig. 1. SEM images of surface morphology of: (a) PZn; (b) PznCo; (c) PZn2Co; (d) PZn3Co; and (e) PZn4Co developed on steel substrate.

with the following reaction; in this case hopeite grains are formed [28]:

$$Zn^{2+} + 2PO_4^{3-} + 4H_2O \rightarrow Zn_3(PO_4)_2 \cdot 4H_2O\downarrow . \quad (4)$$

In general, for samples containing cobalt ions, it can be stated that when a metal substrate with a lower electrode standard potential is immersed in a solution containing cations with a high standard electrode standard, a noble metal can be spontaneously reduced on the metal with a more negative electrode potential. In this case, the reduction potential of cobalt and iron ions is as in formulas (5) and (6), respectively:

$$Co^{2+} + 2e^- = Co \quad E = E^0 + 0.0259 \log\left[Co^{2+}\right], \quad (5)$$

$$Fe^{2+} + 2e^- = Fe \quad E = E^0 + 0.0259 \log\left[Fe^{2+}\right]. \quad (6)$$

There, the cobalt and iron reduction potential is –0.24 and –0.44, respectively. Hence, it can be concluded that the following reaction is carried out spontaneously [29]:

$$Co^{2+} + Fe \rightarrow Fe^{2+} + Co. \quad (7)$$

As a result, this makes it easier to dissolve the substrate and, according to the above reaction, phosphate anions increase. In addition, a higher reduction potential of cobalt ions than zinc ions leads to the stabilization of zinc ions in the solution, which accelerates the process of the formation of the hopeite phase [1]. The XRD analysis of phase composition of PCCs is shown in Fig. 2. Based on the obtained results, the crystals of hopeite (a hydrated zinc phosphate with formula $Zn_3(PO_4)_2 \cdot 4H_2O$) and phosphophyllite with formula $Zn_2Fe(PO_4)_2 \cdot 4H_2O$) were created on the metal surface. It was shown elsewhere, hopeite crystals are likely to be plate-shaped. Since PCC containing 3 g/lit of cobalt ions has the highest amount of hopeite based on the obtained results, it is followed that it has a plate-shaped and dense structure. Therefore, a decrease in the volume percentage of phosphophyllite for PCC leads to a decrease in the dissolution of the metal substrate. The size of phosphate crystals (τ) is measured according to equation (8) [30]:

$$\tau = \frac{K\lambda}{\beta \cos\theta}, \quad (8)$$

where K is the Scherrer constant (0.9), λ is the x-ray wavelength, β is the line length at full-width-half-maximum, and θ is the Bragg angle. Phosphate crystals sizes for PCCs consisting of 1 and 3 g/L Co are 50 and 38 nm, respectively. Thus increasing the amount of an additive by increasing the germination points reduces the size of phosphate crystals. However, the addition of 3 g/L Co to the coating, in comparison with the PCC with 2 and 4 g/L Co additives, increases the size of phosphate crystals and the thickness of the coating, so it can be effective in improving the corrosion resistance of the coating.

Evaluation of Anti-Corrosion Properties of PCCs

Polarization measurements for evaluating the effect of cobalt additive on the corrosion protection

properties of phosphated substrate in a 3.5% NaCl solution are shown in Fig. 3. In addition, the polarization parameters obtained from the Tafel extrapolation method are presented in Table 2. There, it is observed that the anodic and cathodic current densities of PCC with or without additives decrease compared to those of the steel specimen without surface treatment. The most significant decrease in the current density is associated with the PCC sample containing 3 g/L Co additive. Based on these observations, it can be stated that PCC has a greater effect on the reactions performed on the surface. So, when increasing the thickness of PCCs, the density of the cathodic branch decreases. By preventing the metal substrate from dissolving via forming a protective layer through closing the active and accessible anodic areas, the corrosion resistance of the coating increase and the current density of the anodic branch decreases. In fact, the corrosion current density decreases after performing phosphate surface treatment containing an additive. The results showed that the PCC with 3 g/L Co additive has the lowest current density of corrosion.

To sum up, when Co is added, the polarization resistance of the coating improves. In general, PCC with a more density prevents corrosive solution from reaching to the substrate and, as a result, the polarization resistance increases. The samples containing an additive did not change much in the cathodic branch. However, more changes were observed in the anodic branch. These observations indicate that the chemical reaction reduces the anodic reaction rate more than the cathodic reaction rate. The corrosion potential shifts to more positive values after applying the coating due to the formation of a protective layer on the surface of the metal against the corrosive solution [31, 32].

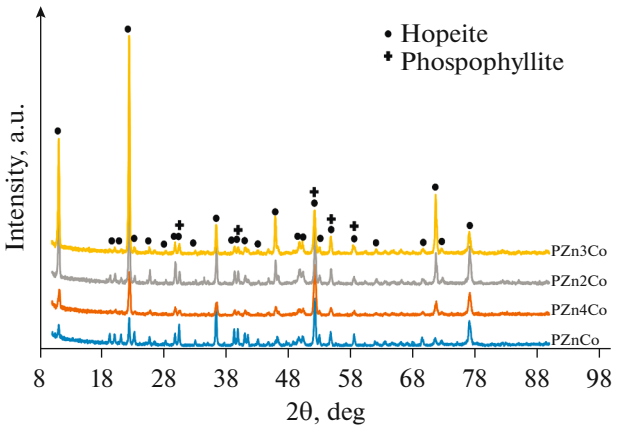

Fig. 2. Phase composition of phosphate coatings analyzed by XRD.

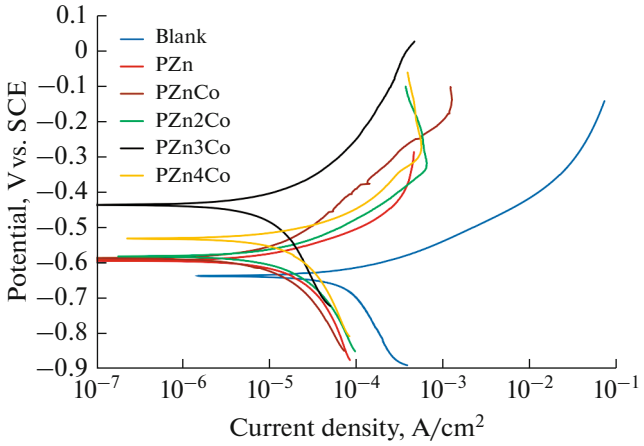

Fig. 3. Polarization curve of phosphated steel substrate samples dipped in 3.5% NaCl solution.

Corrosion Resistance Behavior of Double-Layer Coatings

To evaluate the protective performance and anticorrosion features of epoxy coating, the use of data obtained from the EIS test is a useful method. In this study, the effect of PCC pretreatment containing a cobalt additive on the performance of the top layer in a corrosive solution at the long immersion periods (1, 10, 20, and 30 days) was studied via EIS. The Nyquist and Bode plots are shown in Fig. 4. It is evident from the Bode plots that the samples have two time constants. In other words, as the immersion time passes, the diameters of the semicircles shorten for all specimens. Thus, over time, the electrolyte penetration through the coating and reaching the interface of the coating/substrate will reduce the protective performance of the coating. However, PCCs containing an additive have shown less change over time as a result of the effect of surface preparation on the increased ionic resistance of the coating. In fact, in the samples with PCC pretreatment containing an additive, the amount of penetrated electrolyte during the immersion time of 30 days is much lower than that of untreated steel specimens and the samples with phosphate surface pretreatment. The lowest change in the barrier property, according to Fig. 4, was observed for a sample containing 3 g/L ions of cobalt. The resulting Nyquist curves were fitted to the suitable electrical equivalent circuit. A desirable electrical equivalent circuit for fit-

Table 2. Size of crystals in phosphated coatings with and without Co

Sample	Crystal size, nm
PZn	58
PZnCo	50
PZn2Co	30
PZn3Co	38
PZn4Co	35

Table 3. Polarization parameters extracted via Tafel extrapolation method

Sample	E_{corr}, mV	i_{corr}, μA/cm^2	$-\beta_c$, mV/dec	β_a, mV/dec	R_p
Blank	−645	30	221	85	0.7
PZn	−586	2.4	170	103	9.1
PZnCo	−583	2.2	155	110	10
PZn2Co	−580	2.2	160	119	10.6
PZn3Co	−435	2.0	240	136	14.8
PZn4Co	−531	2.5	215	94	8.9

ting plots is shown in Fig. 5 where, R_s, R_c, R_{ct}, CPE_c, CPE_{dl} and W, represent solution resistance, coating resistance, charge transfer resistance, constant phase element of non-ideal capacity of coating, constant phase element of non-ideal double-layer coating capacity, and the Warburg effect, respectively.

The Warburg effect, due to the discontinuous penetration of the electrolyte, was not observed at the initial time. However, with the lapse of the immersion time, due to an infinite penetration of the corrosive solution through the coating and reaching the interface of the coating/substrate, the effect of Warburg was observed for some samples. The higher resistance for epoxy coatings according to the diameter of the first semi-circle was shown in the Nyquist plots. The depression of the semicircles is caused by their surface non-uniformity and roughness [33]. Electrolyte penetration was affected by the applied epoxy coatings and the ionic resistance of employed surface pretreatment. Therefore, for some samples, the penetration rate is lower, which leads to an increase in the anti-corrosion properties of the epoxy coating. The values of the obtained data from fitting EIS plots are shown in Table 3. As indicated, the lowest values of R_c and R_{ct} are observed for the steel sample. R_c indicates the resistance of the coating against electrolyte penetration through the cavities and flaws of the coating [34]. It also expresses the coating resistance to the penetration of corrosion products released from the metal surface. The degree of the coating resistance, at the beginning, in the surface pretreated samples with and without additive, was higher than that of the blank steel specimen. However, later, usually, the coating resistance diminished so that the lowest change in the coating resistance over time was observed for PCC with 3 g/L Co. In fact, the presence of PCC on the surface of the samples with an optimized structure affects the epoxy coating resistance significantly. The penetration of water through a coating over immersion time probably leads to reduction in the coating resistance of the specimens.

The electrolyte penetration through the epoxy coating affects cross-linking and, with the passage of time, increasing the number of the available pathways to reach the electrolyte to the coating/substrate interface, results in a reduction in the coating barrier properties [35]. As stated there, degradation of the coating because of corrosion sediments causes stress and creates imperfections. In general, with the reduction of the coating barrier properties and the continuous flow of the electrolyte to the substrate, two events may occur. Initially, the hydrolysis of the bonds in the epoxy coating and the less reduction happened. Secondly, cathodic and anodic reactions will begin by reaching the electrolyte and corrosive ions to the coating/substrate interface. Therefore, PCCs, with or without an additive, increase the bond strength of the coating by limiting the electrochemical reactions so that the PCC containing 3 g/L Co, over time, shows the best protection behavior. According to the equivalent electrical circuit, R_{ct} can be used for evaluating the corrosion beneath the coating and adhesion strength [34, 36]. Occurring of cathodic reactions may be more difficult in the presence of surface pretreatment on the surface of a metal and may reduce the rate of lamination. According to the EIS data, the charge transfer resistance for all specimens at the initial times of immersion was high, which it is probably because of the fewer enterings of the electrolyte through the coating, and consequently, the limitation of the reactions in the coating/substrate interface. By the passage of immersion times, the interface of the samples is exposed to more NaCl and R_{ct} decreases. The largest amount of R_{ct} over immersion time has been considered for the PCC containing 3 g/L Co additive. The SEM showed that by adding 3 g/L Co, the coating structure gets more uniform; thus the adhesion of the top layer to the steel improves. As shown in Table 3, the lowest R_{ct} is for the blank steel sample and the PCC sample without an additive. Generally, due to the creation of an obstacle structure on the substrate, PCC reduces the charge transfer resistance of the top layer. But the PCC containing 3 g/L Co additive, due to the creation of a uniform surface structure and limiting the cathodic reactions occurring in the coating/substrate interface, causes an increase in the protective performance of the coating and its barrier properties in the corrosive solution by the passage of time. Due to the depression of Nyquist, for the purpose of converting a constant phase element, the

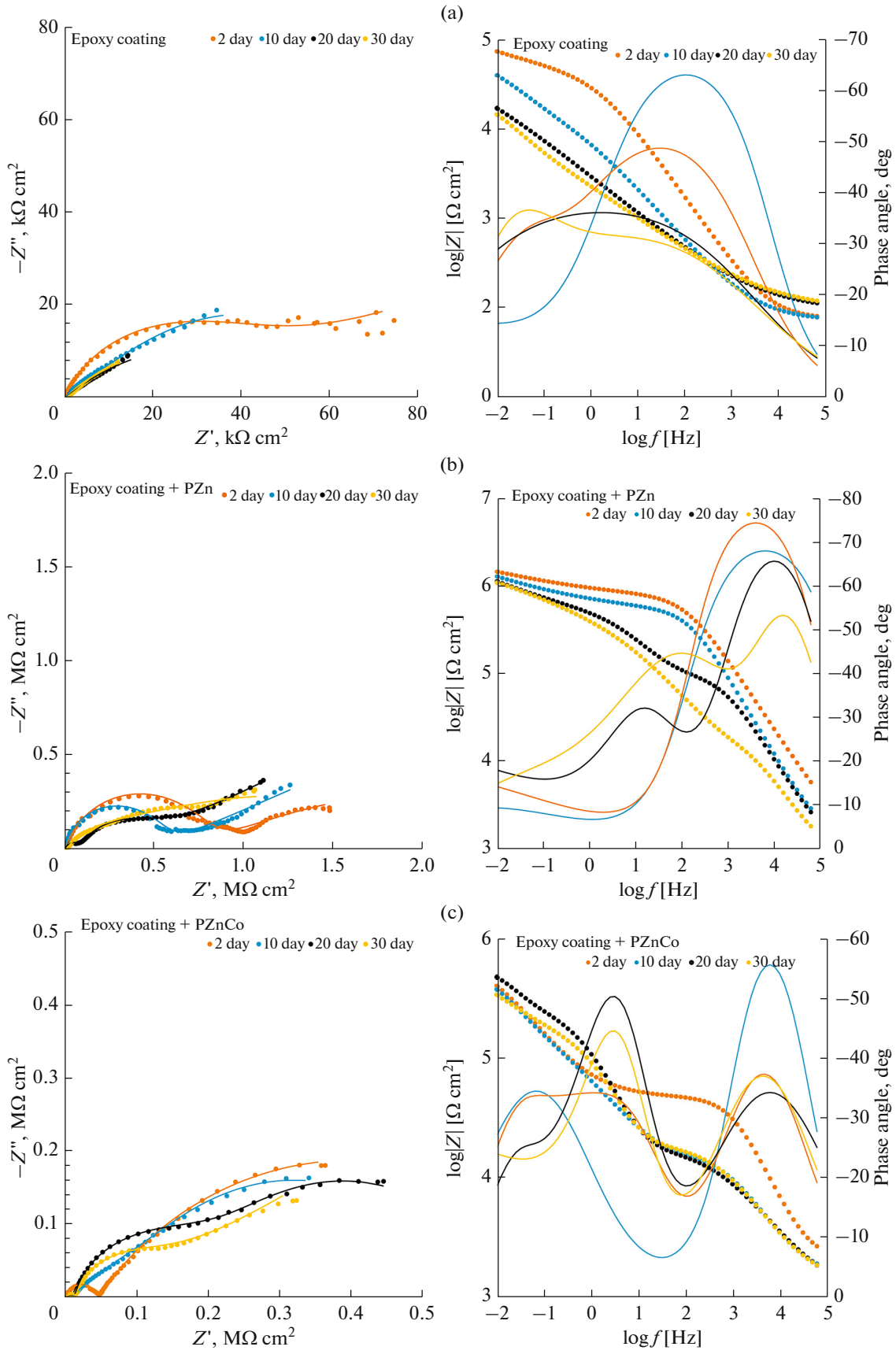

Fig. 4. Nyquist and Bode plots of steel samples with epoxy coatings immersed at different times in 3.5% NaCl solution.

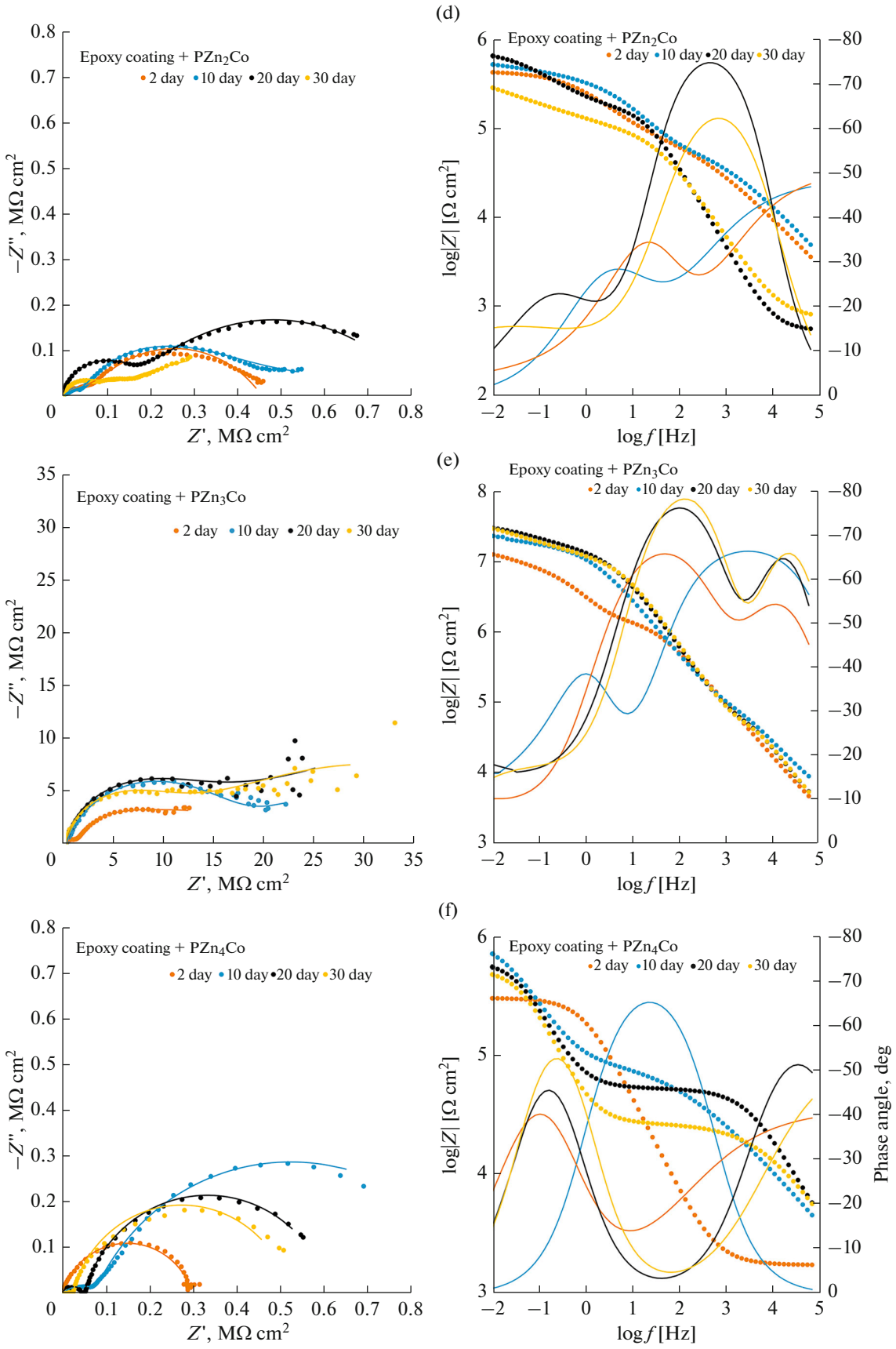
(d)
Epoxy coating + PZn2Co
2 day 10 day 20 day 30 day
−Z'', MΩ cm2
Z', MΩ cm2
log|Z| [Ω cm2]
log f [Hz]
(e)
Epoxy coating + PZn3Co
2 day 10 day 20 day 30 day
−Z'', MΩ cm2
Z', MΩ cm2
log|Z| [Ω cm2]
log f [Hz]
(f)
Epoxy coating + PZn4Co
2 day 10 day 20 day 30 day
−Z'', MΩ cm2
Z', MΩ cm2
log|Z| [Ω cm2]
log f [Hz]
Phase angle, deg

Fig. 4. (Contd.)

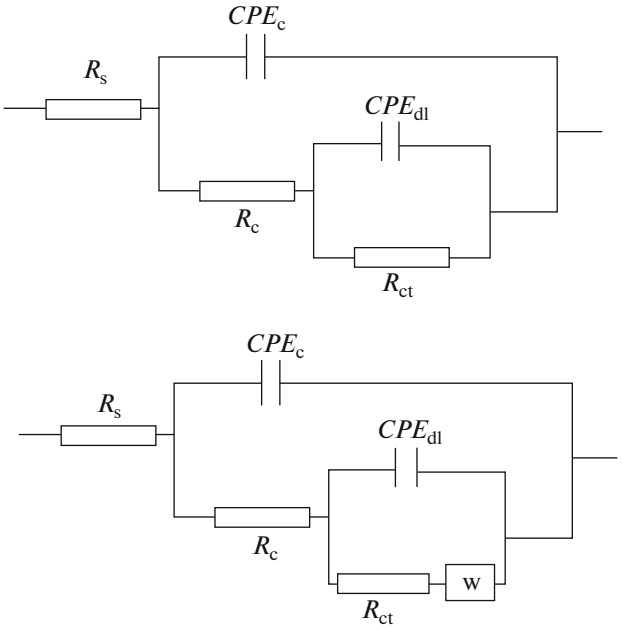

Fig. 5. Equivalent electrical circuit used to obtain electrochemical parameters from Nyquist plots.

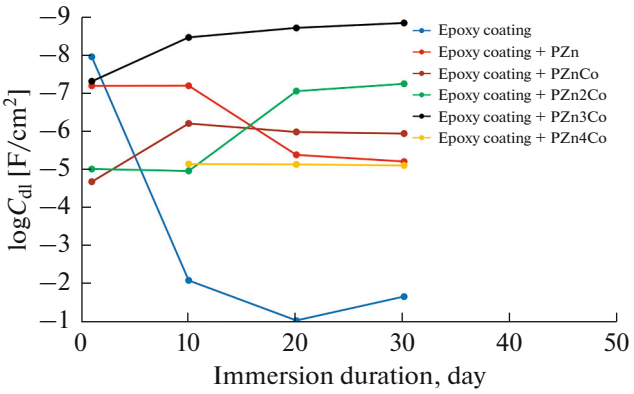

Fig. 6. Coatings capacitance variations over immersion time.

amount of coating and double-layer capacity (C_{coat} and C_{dl}) is calculated by equation (9) [37]:

$$C_x = \frac{(R_x CPE)^{1/n}}{R_x}, \quad (9)$$

where C, CPE, and R, are capacity, a constant phase element, resistance, and n—a frequency dispersion factor, respectively.

The change in C increases the amount of water entering into the coating and the value of C_{dl} indicates the ability to break down the adhesion bond and the electrolyte penetration into the coating/metal interface [38]. The parameter n is influenced by roughness, absorption of inhibition, and formation of porous structure and changes in a range of 0 to 1. Dielectric constant (ε) is affected by the electrolyte penetration into the film [39] and is changed by water penetration (ε for epoxy is approximately 4–8, and for water at ambient temperature it is roughly 80). Thus, the electrolyte penetration into an epoxy layer raises the dielectric constant of epoxy [40]. All of the above mentioned cases related to the dual electric layer are true and, with water penetration, the capacitance of the charge transfer layer increases. The variations of the capacitance of the double electric layer of the coated samples with the passage of immersion time are shown in Fig. 6. Regarding the equation mentioned in [41], the capacitance of a doublel layer, in addition to the constant dielectric and thickness of the transfer layer, is also influenced by the electrolyte. It is shown in Fig. 6 that at the earliest times, the lowest capacitance is related to the sample of PCCs without additives and the PCC containing 3 g/L Co. With the passage of the immersion time, the capacitance of the charge transfer layer for PCCs containing Co additive increases, while it decreases for the additive-free PCCs, which is probably due to the change in dielectric constant and thickness. When the volume of flaws and imperfections in the coating is high, then the double layer capacity increases significantly with the change of a dielectric constant. Also, after a short immersion time in a salty environment, the resistance of the PCC sample without an additive initially increases and then decreases as a result of filling the defects of the coating with the already formed carbon products [42].

These corrosion products result from the dissolution of hopeite. In other words, the dissolution of the PCC reduces the thickness of the coating and its capacitance. It has been revealed that PCC with 3 g/L Co additive absorbs much less water than other specimens over a 30 days immersion period and it demonstrates good protective performance. In general, according to the research results of others, adhesion bond failure and electrolyte penetration to the coating/metal interface are attributed to the change in C_{dl} [43]. Thus, for the PCC containing 3 g/L Co additive, C_{dl} is lower than in other samples. In fact, the density of the steel surface in the presence of 3 g/L Co can improves the resistance of the coating against adhesion degradation; which can, in turn, reduce the lamination rate.

The impedance parameter is presented at a frequency of 10 mHz from the Bode curve as a suitable measure for the evaluation of the protective performance without fitting [13, 44]. In this method, the predicted error occurs more seldom than the results of the fitting procedure. Impedance changes in low fre-

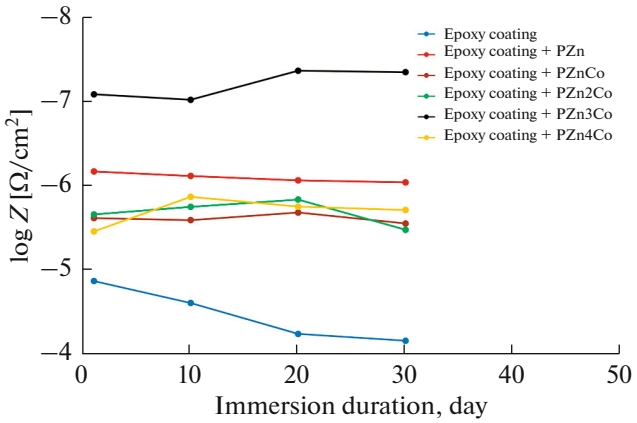

Fig. 7. Impedance module at 0.01Hz frequency for all samples during immersion.

quencies at the immersion time of up to 30 days are shown in Fig. 7. In the early days and at low frequencies, the amount of impedance for all samples is high. This observation indicates that in the early times, due to a lower electrolyte penetration, the protective properties of the epoxy coating are acceptable. Additionally, the impedance for the samples containing an additive is larger than that of the steel coated with epoxy at low frequencies. In the present study it was found that the impedance rate for all samples tended to decrease over time, but, for the specimen of PCC with 3 g/L Co additive, the impedance at low frequencies increased over time. Therefore, in general, PCCs, through increasing the coating corrosion resistance according to a dense and uniform structure, postpone the penetration of the corrosive electrolyte. In addition, by creating a conversion coating layer, the necessary locations for the cathodic reaction and the formation of hydroxyl ions are reduced. The formed conversion coating limits active sites for electrochemical reactions; thus lower hydrolysis of adhesion bonds and corrosion products are created. Samples with more resistance show a higher phase angle [45] and more capacitive electrochemical behavior [46]. The phase angle for all specimens at the initial times had the lowest value, while, with the lapse of time, the lowest amount of phase angle changes was registered in the PCC with 3 g/L Co. Therefore, a more capacitive behavior is observed for this sample; hence, this coating exhibits resistance to higher charge transfers and better adhesion to the epoxy coatings on the substrate [47]. In fact, the PCC with a cobalt additive (through the control of water penetration into coating/substrate interface and the limitation of active sites for the cathode reaction) leads to improved protective properties and reduced degradation.

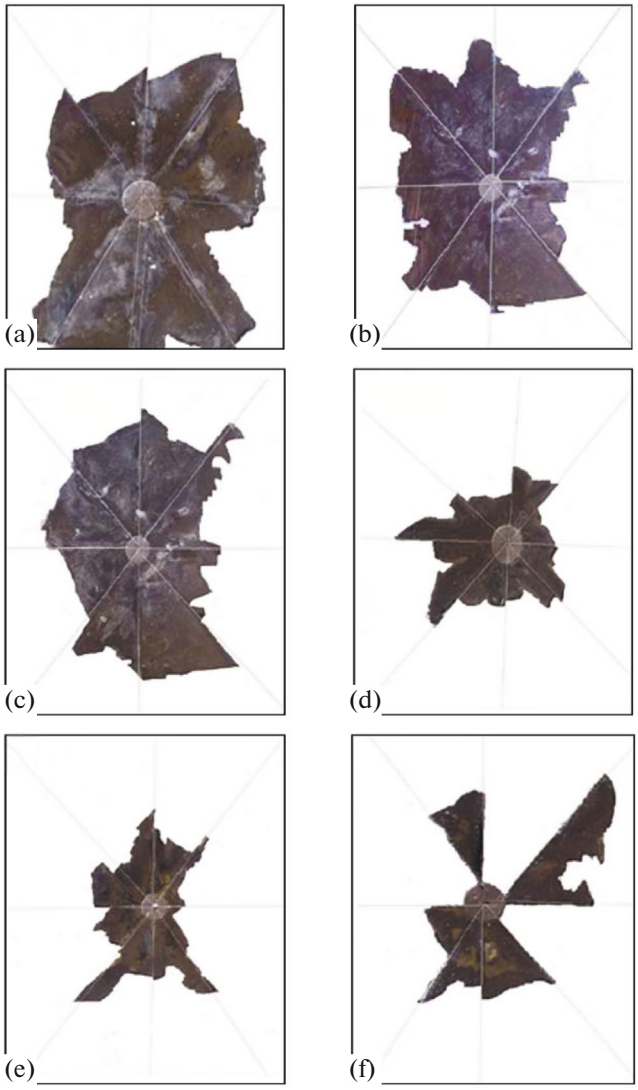

Fig. 8. Disbonded radius of epoxy coatings: (a) without surface pretreatment; (b) with PZn; (c) with PZnCo; (d) with PZn2Co; (e) with PZn3Co; and (f) with PZn4Co, after 60 h immersion.

Measurements of Cathodic Disbondment

The cathodic disbondment test was conducted to investigate the influence of the surface pretreatment of PCC with and without an additive on both blank steel and coated samples (Fig. 8). The results showed the radius of cathodic disbondment for the PCC samples was reduced and the lowest cathodic disbondment was observed for the PCC sample saturated with 3 g/L Co. Meanwhile, with increasing the immersion time, for the mentioned sample, the cathodic disbondment rate did not change consi-derably. It has been shown that the cathodic disbondment resistance of organic coatings strongly depends on the surface preparation; therefore, several reasons such as the formation of

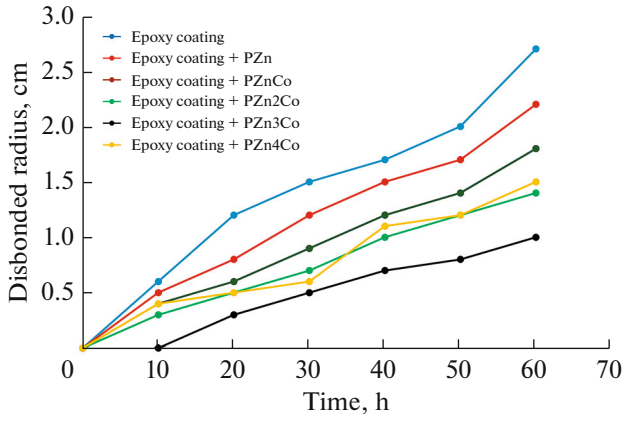

Fig. 9. Disbondment radius vs time in 60 h immersion.

more hydrogen bonds between the epoxy polar groups and the available oxygen in the surface pretreatment can be effective through creating more mechanical locking and physical bonding of the coating with the substrate. According to Fig. 9, at the initial immersion time, the disbondment rate for all samples is negligible; however, the imposed cathodic current increases the isolated region and, as a result, cathodic reactions increase. Also by increasing the pH, the adhesion strength decreases [48, 49]. Regarding the obtained results, applying surface treatment on the substrate decreases the cathodic disbondment radius in comparison with that of the untreated steel substrate. However, PCCs are exposed to more electrolyte due to their porous structure; thus the cathodic reactions increased. Therefore, based on the research carried out elsewhere, the formed hopeite phase is not stable with increasing pH and this PCC cannot signifi-cantly change the cathodic disbondment resistance [50]. It is reported that a double-layer coating with 3 g/L Co shows the lowest cathodic disbondment at a certain immersion time (e.g., 60 hours). This coating, by creating a more uniform and denser structure through preventing the pH local increase, reduces the cathodic disbondment [51]. In addition, in the research presented in [49], it was observed that PCC had the capability to adsorb a hydroxyl ion and reduce the disbondment, indicating that the strong adhesion of the epoxy coating to the substrate is achieved through PCC pretreatment [52]. Also the cathodic sites on the surface are diminished after PCC and the concentration of OH^- around the pores and beneath the film decreases.

Adhesion Strength Measurements by Pull-off

The amount of cavities and porosity inside the epoxy coating is increased by exposure to corrosive solutions, which, in turn, leads to easier electrolyte penetration into the epoxy coating [53]. Hydrolysis occurs in adhesion bonds, resulting in the disbondment of the coating and the spread of corrosion products under the coating. In fact, due to the cathodic reaction and production of a hydroxyl ion, the disbondment rate increases [54]. Accordingly, in the present research, the adhesion strength properties of the coatings in a dry state and after 14 days of immersion were studied in a 3.5% NaCl solution (Table 5). Then the lack of adhesion was calculated by equation (10) borrowed from [55]:

$$\text{Adhesion loss } (\%) = \frac{\text{Dry adhesion strength} - \text{Wet adhesion strength}}{\text{Dry adhesion strength}}. \quad (10)$$

According to Table 4, the lack of adhesion for the top layer of a double-layer coating on the phosphate treated samples containing an additive is less than that of a single layer coating. However, it is evident that the lowest lack of adhesion is for the PCC containing 3 g/L Co. Generally, as to the amount of adhesion lack, the PCC (as a surface pretreatment) prevents the reduction of adhesion strength in the wet state in two ways [56, 57]: initially, it delays the entering of a corrosive electrolyte through improving mechanical inter-locking between the film and steel metal. Second, by formation of an obstacle film at the interface, the locations for cathodic reactions and the formation of hydroxyl ions are reduced. Thus, the formed conversion coating limits active regions for the electrochemical reactions under the coating; this results in lower hydrolysis of the adhesion bonds and less corrosion products. In fact, PCC without an additive, due to having more active locations for the cathodic reaction (more porosity), reduces the coating adhesion strength.

CONCLUSIONS

In this research, the effect of PCC pretreatment with and without cobalt additive on the anti-corrosion properties of the top layer (an epoxy layer applied on steel) was studied. According to the SEM and XRD results, PCC has a lower porosity and a more uniform structure with lower cracks. Also the crystals formed

Table 4. Data obtained from fitting of Nyquist plots with Zview2 software

Sample	Time, day	R_s, $\Omega\ cm^2$	R_c, $\Omega\ cm^2$	CPE_c, $\Omega^{-1}\ cm^{-2}\ s^n$	n_1	R_{ct}, $\Omega\ cm^2$	CPE_{dl}, $\Omega^{-1}\ cm^{-2}\ s^n$	n_2
Blank steel	2	500	28935	4.3×10^{-6}	0.76	44523	3.9×10^{-6}	0.23
	10	90	15624	5.5×10^{-5}	0.61	24875	1×10^{-3}	0.61
	20	77	1126	1.5×10^{-5}	0.42	16132	1.4×10^{-3}	0.43
	30	97	5000	1.9×10^{-5}	0.71	9278	4.5×10^{-3}	0.71
PZn	2	2750	99852	2.4×10^{-7}	0.54	349867	2.4×10^{-7}	0.65
	10	2600	75930	1.2×10^{-7}	0.57	424258	1.3×10^{-7}	0.8
	20	550	170660	7.4×10^{-8}	0.9	522884	3×10^{-6}	0.6
	30	470	88558	1.4×10^{-7}	0.8	112430	7.9×10^{-6}	0.31
PZnCo	2	2250	45948	1.1×10^{-8}	0.86	370154	9.1×10^{-6}	0.6
	10	1971	15875	1.5×10^{-7}	0.7	377960	6.6×10^{-7}	0.95
	20	1877	17548	4.6×10^{-7}	0.59	465021	1.1×10^{-6}	0.9
	30	1880	18389	2.5×10^{-7}	0.66	204050	1.3×10^{-6}	0.9
PZn2Co	2	5863	755290	5.4×10^{-9}	0.8	799470	2.3×10^{-6}	0.3
	10	2925	483050	4.1×10^{-9}	0.89	685210	2.4×10^{-6}	0.25
	20	2627	98019	6.9×10^{-9}	0.86	706365	1.8×10^{-7}	0.74
	30	1824	16870	1.2×10^{-8}	0.85	499875	1.7×10^{-7}	0.69
PZn3Co	2	5037	1730700	1.1×10^{-8}	0.77	10717300	5×10^{-8}	0.95
	10	9600	150000	6.3×10^{-9}	0.77	20084000	5.7×10^{-9}	0.81
	20	5576	86229	1.4×10^{-9}	0.92	23709770	2.4×10^{-9}	0.93
	30	5544	79356	1.4×10^{-9}	0.91	21626640	1.6×10^{-9}	0.97
PZn4Co	2	1690	365600	7.7×10^{-7}	0.81			
	10	4393	93168	5.6×10^{-7}	0.46	646420	4.9×10^{-6}	0.76
	20	5836	51579	1.1×10^{-8}	0.76	412160	6×10^{-6}	0.83
	30	5500	27489	8.8×10^{-8}	0.57	487430	6.3×10^{-6}	0.85

Table 5. Adhesion strength measured in dry and wet modes after 14 days of immersion

Sample	Dry adhesion, MPa	Wet adhesion, MPa	Adhesion loss, %
Blank	2 ± 0.25	1.1 ± 0.25	45
PZn	2.15 ± 0.2	1.4 ± 0.2	35
PZnCo	2.5 ± 0.1	1.8 ± 0.2	28
PZn2Co	2.6 ± 0.2	2.2 ± 0.15	15
PZn3Co	2.7 ± 0.05	2.4 ± 0.1	11
PZn4Co	2.55 ± 0.1	2.15 ± 0.2	16

on the surface for the PCC with cobalt additive deformed to the plate shape. In fact, this additive changed the shape and size of the crystals. Potentiodynamics polarization results showed that the PCC improves the corrosion resistance through the transfer of corrosion potential to more positive values and decreases the corrosion current density. The modification of PCC pretreatment properties leads to better protective performance and higher adhesion strength of the top layer. The anti-corrosion properties of double-layer coatings obtained from EIS increased over time for the samples of PCC containing an additive. Additionally, the adhesion strength increased for these specimens and the least lack of adhesion was for the

PCC having 3 g/L Co. PCC pretreatment by limiting the sites of the cathodic reaction and preventing electrolyte penetration reduced the rate of cathodic disbondment during the immersion time. Also, increasing the adhesion strength of the top layer because of PCC pretreatment is effective in improving cathodic disbondment resistance.

REFERENCES

1. Golabadi, M., Aliofkhazraei, M., Toorani, M., et al., *J. Ind. Eng. Chem.*, 2017, vol. 47, pp. 154–168.
2. Golabadi, M., Aliofkhazraei, M., Toorani, M., et al., *Prog. Org. Coat.*, 2017, vol. 105, pp. 258–266.
3. Harun, M., Marsh, J., and Lyon, S., *Prog. Org. Coat.*, 2005, vol. 54, no. 4, pp. 317–321.
4. Bajat, J., Mišković-Stanković, V., Bibić, N., et al., *Prog. Org. Coat.*, 2007, vol. 58, no. 4, pp. 323–330.
5. Bajat, J., Mišković-Stanković, V., Popić J., et al., *Prog. Org. Coat.*, 2008, vol. 63, no. 2, pp. 201–208.
6. Vaca-Cortés, E., Lorenzo, M.A., Jirsa, J.O., et al., *Adhesion Testing of Epoxy Coating: Research Report No. 1265-6*, Austin, TX: Univ. of Texas, 1998, pp. 1–129.
7. Zhang, X., Sloof, W., Hovestad, A., et al., *Surf. Coat. Technol.*, 2005, vol. 197, no. 2, pp. 168–176.
8. Deflorian, F., Rossi, S., Fedrizzi, L., et al., *Prog. Org. Coat.*, 2005, vol. 52, no. 4, pp. 271–279.
9. Bamoulid, L., Maurette, M.-T., De Caro, D., et al., *Surf. Coat. Technol.*, 2008, vol. 202, no. 20, pp. 5020–5026.
10. Palraj, S., Selvaraj, M., and Jayakrishnan, P., *Prog. Org. Coat.*, 2005, vol. 54, no. 1, pp. 5–9.
11. Freeman D.B., *Phosphating and Metal Pre-treatment: A Guide to Modern Processes and Practice*, New York: Industrial Press, 1986, 1st ed.
12. Lin, B.-L., Lu, J.-T., and Kong, G., *Surf. Coat. Technol.*, 2008, vol. 202, no. 9, pp. 1831–1838. https://doi.org/10.1016/j.surfcoat.2007.08.001
13. Akhtar, A., Susac, D., Glaze, P., et al., *Surf. Coat. Technol.*, 2004, vol. 187, no. 2, pp. 208–215.
14. Song, Y. and Mansfeld, F., *Corros. Sci.*, 2006, vol. 48, no. 1, pp. 154–164.
15. Zimmermann, D., Munoz, A., and Schultze, J., *Electrochim. Acta*, 2003, vol. 48, no. 20, pp. 3267–3277.
16. Zarei, A. and Afshar, A., in *Proc. TMS 2009 Annual Meeting and Exhibition*, San Francisco, 2009, no. 1, pp. 615–623.
17. Tsai, C.-Y., Liu, J.-S., Chen, P.-L., et al., *Corros. Sci.*, 2010, vol. 52, no. 10, pp. 3385–3393. https://doi.org/10.1016/j.corsci.2010.06.020
18. Li, G., Niu, L., Lian, J., et al., *Surf. Coat. Technol.*, 2004, vol. 176, no. 2, pp. 215–221.
19. Sandu, A.V., Ciomaga, A., Nemtoi, G., et al., *Microsc. Res. Techn.*, 2012, vol. 75, no. 12, pp. 1711–1716.
20. Sandu, A., Ciomaga, A., Nemtoi, G., et al., *J. Optoelectron. Adv. Mater.*, 2012, vol. 14, no. 7, p. 704.
21. Sandu, A.V., Bejinariu, C., Nemtoi, G., et al., *Rev. Chim.*, 2013, vol. 64, no. 8, pp. 825–827.
22. Akhtar, A., Susac, D., Wong, K., et al., *Mater. Sci. Forum*, 2006, vols. 519–521, pp. 753–758. https://doi.org/10.4028/www.scientific.net/MSF.519-521.753
23. Banczek, E., Rodrigues, P., and Costa, I., *Surf. Coat. Technol.*, 2007, vol. 202, no. 10, pp. 2008–2014.
24. Cho, K., Rao, V.S., and Kwon, H., *Electrochim. Acta*, 2007, vol. 52, no. 13, pp. 4449–4456.
25. Shin, A. and Shon, M., *J. Ind. Eng. Chem.*, 2010, vol. 16, no. 6, pp. 884–890.
26. Ghanbari, A. and Attar, M., *Appl. Surf. Sci.*, 2014, vol. 316, pp. 429–434.
27. Kumar, A., Bhola, S., and Majumdar, J.D., *Surf. Coat. Technol.*, 2012, vol. 206, no. 17, pp. 3693–3699.
28. Su, H.-Y. and Lin, C.-S., *Corros. Sci.*, 2014, vol. 83, pp. 137–146. https://doi.org/10.1016/j.corsci.2014.02.002
29. Pourbaix, M., *Atlas of Electrochemical Equilibria in Aqueous Solutions*, Houston, TX: Natl. Assoc. Corros. Eng., 1974.
30. D'Agostino, A.T., *Anal. Chim. Acta*, 1992, vol. 262, no. 2, pp. 269–275.
31. Umoren, S. and Gasem, Z., *J. Dispersion Sci. Technol.*, 2014, vol. 35, no. 8, pp. 1181–1190.
32. de Freitas Cunha Lins, V., de Andrade Reis, G.F., de Araujo, C.R., and Matencio, T., *Appl. Surf. Sci.*, 2006, vol. 253, no. 5, pp. 2875–2884.
33. Popova, A., Raicheva, S., Sokolova, E., et al., *Langmuir*, 1996, vol. 12, no. 8, pp. 2083–2089.
34. Ramezanzadeh, B. and Attar, M., *Mater. Chem. Phys.*, 2011, vol. 130, no. 3, pp. 1208–1219.
35. Romagnoli, R. and Vetere, V., *Corrosion*, 1995, vol. 51, no. 2, pp. 116–123.
36. Rosalbino, F., Scavino, G., Mortarino, G., et al., *J. Solid State Electrochem.*, 2011, vol. 15, no. 4, pp. 703–709.
37. Song, G.-L. and Shi, Z., *Corros. Sci.*, 2014, vol. 85, pp. 126–140. https://doi.org/10.1016/j.corsci.2014.04.008
38. Negm, N.A., Kandile, N.G., Badr, E.A., et al., *Corros. Sci.*, 2012, vol. 65, pp. 94–103.
39. Markhali, B., Naderi, R., Mahdavian, M., et al., *Corros. Sci.*, 2013, vol. 75, pp. 269–279.
40. Hosseini, M., Jafari, M., and Najjar, R., *Surf. Coat. Technol.*, 2011, vol. 206, no. 2, pp. 280–286.
41. Hanza, A.P., Naderi, R., Kowsari, E., et al., *Corros. Sci.*, 2016, vol. 107, pp. 96–106.
42. Lu, X., Blawert, C., Huang, Y., et al., *Electrochim. Acta*, 2016, vol. 187, pp. 20–33.
43. van der Weijde, D., van Westing, E., and De Wit, J., *Corros. Sci.*, 1994, vol. 36, no. 4, pp. 643–652.
44. Zand, B.N. and Mahdavian, M., *Electrochim. Acta*, 2007, vol. 52, no. 23, pp. 6438–6442.

45. Naderi, R. and Attar, M., *Corros. Sci.*, 2009, vol. 51, no. 8, pp. 1671–1674.

46. Naderi, R., Mahdavian, M., and Attar, M., *Electrochim. Acta*, 2009, vol. 54, no. 27, pp. 6892–6895.

47. Alibakhshi, E., Ghasemi, E., and Mahdavian, M., *Prog. Color, Color. Coat.*, 2012, vol. 5, pp. 91–99.

48. Grundmeier, G. and Stratmann, M., *Annu. Rev. Mater. Res.*, 2005, vol. 35, pp. 571–615.

49. Ogle, K., Morel, S., and Meddahi, N., *Corros. Sci.*, 2005, vol. 47, no. 8, pp. 2034–2052.

50. Ramezanzadeh, B. and Rostami, M., *Appl. Surf. Sci.*, 2017, vol. 392, pp. 1004–1016.

51. Naderi, R. and Attar, M., *Corros. Sci.*, 2010, vol. 52, no. 4, pp. 1291–1296.

52. Sørensen, P.A., Dam-Johansen, K., Weinell, C., et al., *Prog. Org. Coat.*, 2010, vol. 68, no. 1, pp. 70–78.

53. Heydarpour, M., Zarrabi, A., Attar, M., et al., *Prog. Org. Coat.*, 2014, vol. 77, no. 1, pp. 160–167.

54. Alibakhshi, E., Ghasemi, E., Mahdavian, M., et al., *Corros. Sci.*, 2017, vol. 115, pp. 159–174.

55. Askari, F., Ghasemi, E., Ramezanzadeh, B., et al., *Prog. Org. Coat.*, 2015, vol. 85, pp. 109–122.

56. van den Brand, J., van Gils, S., Beentjes, P., et al., *Prog. Org. Coat.*, 2004, vol. 51, no. 4, pp. 339–350.

57. McCafferty, E., *J. Adhes. Sci. Technol.*, 2002, vol. 16, no. 3, pp. 239–255.